Acta Cryst. (1979). B**35**, 2836–2842

Structural Features of $Nb_{1-x}Ti_xO_2$

BY KIMIKO SAKATA

National Research Institute for Metals, Meguro-ku, Tokyo 153, *Japan*

(*Received* 27 *March* 1979; *accepted* 9 *July* 1979)

Abstract

X-ray structural analysis with Mo $K\alpha$ radiation was carried out for $Nb_{1-x}Ti_xO_2$ ($0 \le x \le 0{\cdot}2$) in its low-temperature deformed rutile phase $I4_1/a$. Crystals were prepared by chemical transport, with $TeCl_4$ as the transport agent. Atomic parameters determined for NbO_2 are in good agreement with those obtained by neutron diffraction. For superlattice reflections with h, $k = 2n + 1$ and $l = 2n$ in the system $Nb_{1-x}Ti_xO_2$, the discrepancy between F_o and F_c is appreciable. Attempts to clarify this situation are made and discussed. Analysis of interatomic distances for NbO_2 showed that Nb—Nb pair bonds exist along z and strong Nb—O—O—Nb bonds exist along x and y in the form of non-intersecting linear chains. With such a molecular-chain model the structural features and phase transition in the $Nb_{1-x}Ti_xO_2$ system are discussed.

Introduction

NbO_2 undergoes a phase transition at around 1073 K, which is, in all respects, akin to that for VO_2 at 341 K (Sakata, Sakata & Nishida, 1967; Sakata, 1969*a*). The high-temperature (HT) phase has a simple rutile-type structure (space group $P4_2/mnm$) and the low-temperature (LT) phase a slightly deformed one, characterized by a series of superlattice reflections on an X-ray diffraction pattern. The space group has been identified to be $I4_1/a$ through X-ray experiments (Magnéli, Andersson & Sundkvist, 1955). The reflections for the LT phase have been indexed and atomic positions have been given by Marinder (1963). Recently, an accurate redetermination of all the atomic parameters has been carried out by neutron diffraction (Pynn, Axe & Thomas, 1976; hereafter PAT, 1976).

Moreover, the structural fluctuations associated with the phase transition have been studied by inelastic neutron scattering (Shapiro, Axe, Shirane & Raccah, 1974; Pynn & Axe, 1976; Pynn, Axe & Raccah, 1978). The structural phase transition in NbO_2 is associated with relatively small changes in thermal, electrical and magnetic properties in comparison with the drastic changes in the isoelectronic VO_2 (Rüdorff & Luginsland, 1964; Janninck & Whitmore, 1966; Sakata, 1969*b*; Rao, Rama Rao & Subba Rao, 1973). Recently, with large single crystals, the Hall effect, electrical conductivity and thermoelectric power were measured along c (Bélanger, Destry, Perluzzo & Raccah, 1974). The experiment on electrical conductivity *vs* temperature has clearly revealed the semiconductor-to-metal transition. In the LT phase Nb—Nb distances are alternately shorter and longer along c. The structural phase transition is taken to correspond to the thermal dissociation of the shorter Nb—Nb bonds, which will give a non-paired $4d$ electron on each Nb^{4+} ion, responsible for the change in conduction and paramagnetism.

The substitutional system $Nb_{1-x}Ti_xO_2$ ($0 \le x \le 0{\cdot}1$) behaves much like pure NbO_2, and undergoes a structural phase transition at 1073 ~ 873 K (Sakata, 1969*c*). This system has been of interest because the dissociation of Nb—Nb dimers is expected to be brought about by the substitution of Ti for Nb ions (Rüdorff & Luginsland, 1964; Sakata, Nishida, Matsushima & Sakata, 1969). In fact, the structural distortion of the LT phase disappears when $x > 0{\cdot}17$ (Shin, Halpern & Raccah, 1975).

With an automatic four-circle diffractometer and monochromatic Mo $K\alpha$ radiation, the structural modification in $Nb_{1-x}Ti_xO_2$ ($0 \le x \le 0{\cdot}2$) is studied in the present report. Attempts are made to clarify the origin of the discrepancies between the observed and calculated structure factors for the hkl and khl reflections (PAT, 1976). In terms of a molecular chain obtained by joining the shortest interatomic distances in $Nb_{1-x}Ti_xO_2$ the structural phase transition is discussed.

Experimental details

(*a*) *Crystal preparation*

Single crystals of $Nb_{1-x}Ti_xO_2$ were prepared by chemical transport using $TeCl_4$ (Sakata, Sakata, Höfer & Horiuchi, 1972). Weighed amounts of NbO_2 and TiO_2 powders were intimately mixed and heated in an evacuated quartz tube for 72 h. The solid-solution powders of $Nb_{1-x}Ti_xO_2$ thus obtained were used as the starting materials for the transport. Crystals were prepared in the composition range $0 \le x \le 0{\cdot}5$. Their cell

0567-7408/79/122836-07$01.00

Table 1. *Composition and lattice parameters* (Å) *of the* $Nb_{1-x}Ti_xO_2$ *single crystals used for the diffraction intensity measurements*

Composition	Lattice parameter (Å)	
x	a	c
0·00	13·695 (2)	5·981 (1)
0·04	13·666 (10)	5·997 (12)
0·09	13·632 (30)	5·971 (8)
0·20	13·559 (33)	5·998 (15)

dimensions were determined on the diffractometer with Mo $K\alpha$ radiation monochromated with graphite. From the lattice parameter *vs* composition curve, determined for the pre-transport powders, compositions for the single crystals obtained were estimated. The deviations of composition x in the single crystals from that in the corresponding starting material were found to be within 1%.

Crystals grown on the lower-temperature wall of the reaction tube were octahedral, and many of them were twinned. Good crystals were observed to be bounded by the (402) planes [corresponding to the (221) planes of the basic rutile lattice]. The residues of the starting material in the higher-temperature region of the reaction tube were observed to be transformed into fine octahedral crystallites. The compositions and lattice parameters of the single-crystal specimens used are shown in Table 1.

(*b*) *Collection and reduction of data*

Intensities were collected on a Philips PW 1100 automatic four-circle diffractometer with Mo $K\alpha$ radiation monochromated by graphite. The crystals were ground into spheres about 0·15 mm in diameter. An ω–2θ scan mode was used at a rate of 4° min^{-1}. Background counts for 10 s were measured at each end of the scan range $\Delta\omega$, which was increased with ω according to $\Delta\omega = (\alpha + 0{\cdot}5 \tan\theta)°$. High-quality crystals were selected from those which showed sharp reflection spots on an oscillation photograph. However, for certain compositions, the photograph showed broad diffraction patterns. In such samples the value of α was chosen in the range 1·8 ~ 3·0°. To check the stability of the diffractometer and the crystal setting, three standard reflections were measured every 120 min. The fluctuations in integrated intensities over three days were within 0·2%. The intensities were corrected for Lorentz and polarization effects, but not for absorption. The reflections were collected in a scanning range $3 < \theta < 40°$ from those having indices $0 \le h \le 25$, $0 \le k \le 25$ and $0 \le l \le 10$. The numbers of independent $|F_o|$'s obtained for $x = 0$, 0·04, 0·09 and 0·20 were 2189, 2825, 2051 and 2162, respectively; $|F_o|$'s for equivalent reflections were averaged.

(*c*) *Structure refinements*

The LT (below 1073 K) phase of NbO_2, as well as titanium-modulated niobium oxide, $Nb_{1-x}Ti_xO_2$ ($x \le 0{\cdot}2$), belongs to the space group $I4_1/a$. The unit cell is composed of 16 slightly distorted subcells of rutile-type structure and contains 96 atoms. However, the specification of the coordinates of two metal atoms, $M(1)$ and $M(2)$, as well as four O atoms, O(1), O(2), O(3) and O(4), is sufficient to describe them. The position of an atom with respect to the LT-phase coordinate system is denoted by (x,y,z). Then the general atomic position commensurate with the space group $I4_1/a$ of the LT phase (x,y,z) is a member of the symmetry-related set: (0,0,0) and $(\frac{1}{2},\frac{1}{2},\frac{1}{2})$ plus (x,y,z); $(\bar{x}, \frac{1}{2}-y, z)$; $(\frac{3}{4}-y, \frac{1}{4}+x, \frac{1}{4}+z)$; $(\frac{1}{4}+y, \frac{1}{4}-x, \frac{1}{4}+z)$; $(\bar{x},\bar{y},\bar{z})$; $(x, \frac{1}{2}+y, \bar{z})$; $(\frac{1}{4}+y, \frac{3}{4}-x, \frac{3}{4}-z)$; $(\frac{3}{4}-y, \frac{3}{4}+x, \frac{3}{4}-z)$.

Refinements were accomplished with the full-matrix least-squares program *MINEPAC* to minimize $\sum ||F_o| - |F_c|| / \sum |F_o|$.

Atomic parameters were determined for the system $Nb_{1-x}Ti_xO_2$, x = 0·00, 0·04, 0·09 and 0·20. The results were compared with those obtained by neutron diffraction (PAT, 1976) (§ $c-1$).

It was noticed that there was a systematic discrepancy between F_o and F_c for all the weak superlattice reflections. Such a discrepancy can also be observed in the results of Marinder (1963), *e.g.* for the pairs of reflections 11,1,2, 1,11,2; 13,1,2, 1,13,2; and 15,1,2, 1,15,2, and is taken to be intrinsic to the NbO_2 crystal. An analysis is proposed in § ($c-2$) to clarify the cause of these discrepancies.

($c-1$) *Refinements for* $Nb_{1-x}Ti_xO_2$

All reflections for $0 \le h \le 25$, $0 \le k \le 25$ and $0 \le l \le 10$ were collected, except strong ones with $\sin\theta/\lambda < 0{\cdot}3$ Å, which were considered to suffer from extinction. Thus, with 1318, 1587, 1551 and 1844 reflections for x = 0·00, 0·04, 0·09 and 0·20, respectively, the refinements were carried out for atomic coordinates and anisotropic temperature factors, assuming statistical occupancy of $M(1)$ and $M(2)$ by $Nb_{1-x}Ti_x$. In the next stage the refinements were repeated to obtain the best fit by varying the occupancy ratio Nb/Ti for $M(1)$ and $M(2)$. In this case corrections were not carried out for absorption or extinction. Results for samples NbO_2, $Nb_{0{\cdot}96}Ti_{0{\cdot}04}O_2$, $Nb_{0{\cdot}91}Ti_{0{\cdot}09}O_2$ and $Nb_{0{\cdot}80}Ti_{0{\cdot}20}$ are summarized in Table 2. The percentages of Ti atoms which occupy $M(2)$ positions were found to be larger by 30, 20 and 14% for x = 0·04, 0·09 and 0·20, respectively, than those which occupy $M(1)$ positions. The anisotropic temperature factors β_{33} are very large.

For NbO_2, the refinement was also carried out by excluding those superlattice reflections (h, $k = 2n+1$, $l = 2n$) for which $|\Delta F| = |F_o| - |F_c|$ was especially large. After correction for an anisotropic temperature

factor for each atom, isotropic extinction corrections were made in the final stage. R converged to 0·038 and the atomic parameters were found to be in good agreement with those obtained by PAT (1976) (Table 3). Exclusion of the superlattice reflections with large ΔF's reduced R but made no significant changes to the atomic coordinates.

(c − 2) *Analysis of movement of atomic positions*

A systematic discrepancy exists between F_o and F_c for superlattice reflections with $h, k = 2n + 1$ and $l = 2n$. In order to clarify the cause of these discrepancies, the following refinements were proposed for $Nb_{0.96}Ti_{0.04}O_2$ which showed the most diffuse scattering amongst the samples investigated. Because our primary interest was to follow the changes of atomic coordinates, in all the refinements which follow an isotropic temperature factor was assumed. Results in this case are given in Table 4 as 'ordinary'. R for each layer is summarized in Table 5 which shows that (1) R is much larger for $l = 2n$ than for $l = 2n + 1$ and (2) R for $h, k = 2n + 1$ is greater than for $h, k = 2n$. Thus, R for superlattice reflections with ($h, k = 2n + 1, l = 2n$) is significantly large, while R with ($h = 2n, k = 2n + 1, l = 2n + 1$) and ($h = 2n + 1, k = 2n, l = 2n + 1$) is small. F_o and F_c for each hkl and khl with $h, k = 2n + 1$ and $l = 2n$ are given in Table 6. As can be seen from this table, $F_c(hkl)$ and $F_c(khl)$ are not equal for this crystal, although $F_o(hkl)$ and $F_o(khl)$ are approxi-

Table 2. *Final atomic coordinates* (×10⁴), *anisotropic temperature factors* (×10⁴) *and occupancy factors* (%) *for* $Nb_{1-x}Ti_xO_2$

Composition x		x	y	z	β_{11}	β_{22}	β_{33}	β_{12}	β_{13}	β_{23}	Occupancy Ti	R
0·00	Nb(1)	1150 (1)	1250 (1)	4757 (3)	4 (3)	2 (3)	56 (11)	0 (2)	1 (1)	1 (1)		
	Nb(2)	1345 (1)	1250 (1)	254 (3)	5 (4)	3 (3)	43 (11)	0 (2)	0 (1)	1 (1)		
	O(1)	9838 (9)	1272 (9)	−93 (22)	11 (4)	6 (4)	−78 (80)	−2 (2)	−12 (8)	1 (7)		0·140
	O(2)	9737 (7)	1267 (8)	4960 (21)	2 (3)	5 (3)	−38 (73)	1 (2)	3 (6)	3 (7)		
	O(3)	2719 (12)	1261 (11)	63 (27)	19 (6)	7 (5)	95 (99)	2 (3)	7 (11)	−7 (10)		
	O(4)	2607 (8)	1250 (9)	5109 (25)	4 (3)	8 (4)	70 (87)	2 (2)	−8 (8)	−14 (9)		
0·04	M(1)	1161 (1)	1251 (1)	4782 (2)	10 (4)	6 (3)	63 (3)	0 (2)	−1 (1)	1 (1)	3·40	
	M(2)	1334 (1)	1250 (1)	230 (2)	12 (4)	7 (3)	65 (3)	0 (2)	0 (1)	−1 (1)	4·60	
	O(1)	9869 (8)	1249 (7)	−73 (14)	15 (4)	12 (3)	37 (22)	0 (2)	−6 (5)	−2 (6)		0·187
	O(2)	9741 (7)	1256 (7)	4967 (14)	10 (4)	10 (3)	49 (23)	0 (2)	3 (5)	3 (5)		
	O(3)	2743 (8)	1257 (7)	33 (15)	11 (4)	11 (3)	60 (26)	0 (2)	0 (5)	−1 (6)		
	O(4)	2638 (8)	1259 (7)	5076 (15)	14 (4)	11 (3)	41 (23)	1 (2)	−2 (5)	−1 (6)		
0·09	M(1)	1168 (1)	1244 (1)	4807 (2)	9 (3)	5 (3)	125 (3)	0 (2)	−1 (1)	−2 (1)	8·05	
	M(2)	1322 (1)	1244 (1)	206 (2)	12 (4)	6 (4)	124 (3)	0 (2)	0 (1)	3 (1)	9·95	
	O(1)	9830 (16)	1226 (17)	−63 (14)	16 (5)	9 (4)	86 (32)	3 (3)	−4 (5)	−2 (4)		0·121
	O(2)	9746 (12)	1219 (15)	4994 (12)	3 (2)	11 (4)	94 (30)	0 (2)	4 (3)	−4 (4)		
	O(3)	2734 (15)	1221 (17)	8 (14)	6 (3)	10 (4)	133 (38)	0 (2)	−2 (4)	6 (5)		
	O(4)	2649 (12)	1225 (17)	5071 (15)	5 (5)	14 (5)	131 (35)	−4 (3)	0 (4)	1 (5)		
0·20	M(1)	1228 (1)	1250 (1)	4947 (3)	21 (4)	6 (2)	122 (2)	0 (2)	−2 (1)	4 (1)	18·56	
	M(2)	1294 (1)	1256 (1)	134 (3)	17 (3)	6 (2)	88 (2)	0 (2)	−15 (1)	1 (1)	21·44	
	O(1)	9811 (5)	1260 (5)	39 (23)	7 (2)	6 (2)	126 (27)	0 (2)	−17 (7)	7 (7)		0·140
	O(2)	9761 (4)	1256 (5)	5041 (21)	2 (1)	12 (2)	91 (23)	1 (1)	−3 (6)	12 (7)		
	O(3)	2734 (6)	1252 (5)	9971 (15)	19 (3)	12 (2)	−51 (13)	−3 (2)	10 (5)	9 (5)		
	O(4)	2687 (7)	1262 (5)	4985 (16)	26 (3)	12 (2)	−43 (14)	−2 (2)	0 (6)	−9 (5)		

The anisotropic temperature factors are given by the expression: $\exp[-(h^2\beta_{11} + k^2\beta_{22} + l^2\beta_{33} + 2hk\beta_{12} + 2hl\beta_{13} + 2kl\beta_{23})]$.

Table 3. *Final atomic coordinates* (×10⁴), *anisotropic temperature factors* (×10⁴) *and the isotropic extinction parameters* (×10⁵) *for* NbO_2

	x	y	z	β_{11}	β_{22}	β_{33}	β_{12}	β_{13}	β_{23}
Nb(1)	1151 (1)	1250 (1)	4758 (3)	3 (1)	2 (1)	10 (6)	0 (1)	0 (1)	−1 (1)
Nb(2)	1344 (1)	1249 (1)	262 (3)	4 (1)	3 (1)	8 (5)	0 (1)	−1 (1)	0 (1)
O(1)	9871 (4)	1269 (5)	−52 (5)	2 (1)	7 (1)	25 (7)	−1 (1)	2 (1)	0 (1)
O(2)	9756 (5)	1268 (5)	4994 (5)	6 (1)	7 (1)	17 (7)	2 (1)	1 (1)	−6 (1)
O(3)	2754 (4)	1267 (5)	9995 (5)	3 (1)	12 (1)	15 (6)	−2 (1)	−4 (1)	−1 (2)
O(4)	2639 (5)	1267 (6)	5072 (6)	6 (1)	11 (1)	25 (7)	2 (1)	−6 (2)	−5 (2)

Extinction parameter 0·1946.

mately equal and the following relationship seems to hold for a given l:

$$F_o(hkl) \simeq F_o(khl) = [F_c(hkl) + F_c(khl)]/2.$$

Table 4. *Atomic coordinates* ($\times 10^4$), *isotropic temperature factors* (Å^2) *and R for the ordinary and subgroup refinements of* $Nb_{0\cdot96}Ti_{0\cdot04}O_2$

		x	y	z	B	R
Ordinary	$M(1)$	1163 (1)	1250 (1)	4784 (2)	0·81 (4)	0·207
	$M(2)$	1336 (1)	1250 (1)	227 (2)	0·87 (4)	
	O(1)	9887 (17)	1226 (15)	−80 (21)	1·47 (32)	
	O(2)	9731 (18)	1232 (15)	4952 (20)	1·43 (32)	
	O(3)	2747 (13)	1258 (12)	34 (16)	0·67 (21)	
	O(4)	2655 (13)	1260 (12)	5065 (16)	0·62 (20)	
Subgroup *hkl*	$M(1)$	1161 (1)	1255 (1)	4773 (3)	0·61 (4)	0·179
	$M(2)$	1337 (1)	1244 (1)	239 (3)	0·66 (4)	
	O(1)	9892 (21)	1215 (16)	−91 (27)	1·03 (36)	
	O(2)	9738 (17)	1226 (21)	4984 (28)	1·45 (46)	
	O(3)	2762 (17)	1247 (15)	48 (21)	0·43 (25)	
	O(4)	2672 (17)	1258 (16)	5048 (21)	0·48 (25)	
khl	$M(1)$	1162 (1)	1245 (1)	4773 (3)	0·62 (4)	0·178
	$M(2)$	1338 (1)	1256 (1)	239 (3)	0·66 (4)	
	O(1)	9831 (17)	1249 (15)	−43 (19)	0·42 (23)	
	O(2)	9752 (15)	1237 (15)	4957 (19)	0·36 (22)	
	O(3)	2713 (28)	1305 (20)	35 (29)	1·51 (50)	
	O(4)	2618 (28)	1272 (20)	5096 (32)	1·56 (48)	

Table 5. *R for each layer of* $Nb_{0\cdot96}Ti_{0\cdot04}O_2$

Index	Layer 0	1	2	3	4	5	6	7	8
h	0·19	0·28	0·17	0·23	0·18	0·19	0·14	0·16	0·15
k	0·19	0·28	0·17	0·23	0·18	0·19	0·14	0·16	0·15
l	0·28	0·07	0·23	0·09	0·21	0·08	0·22	0·06	0·25

Table 6. *Comparison of observed and calculated structure factors between the hkl and khl superlattice reflections with odd h and k* ($l = 2, 4, 6, 8$ *and* 10)

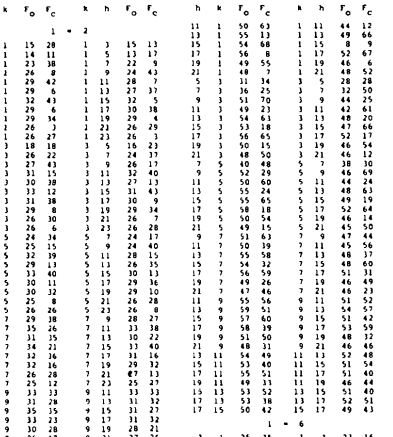

Moreover, $|\Delta F|$ is larger for a larger difference between h and k. These observations are especially marked in $x = 0{\cdot}04$, although they are more or less consistent throughout the system $Nb_{1-x}Ti_xO_2$.

Two independent refinements were carried out for each of two subgroups of reflections, *hkl* and *khl*, giving $R = 0{\cdot}179$ and $0{\cdot}178$, respectively (Table 4). The movements of the y coordinates of $M(1)$ and $M(2)$ are in opposite directions for the *hkl* and *khl* groups. When those reflections for which $F_o \ll F_c$ and $F_o \gg F_c$ were omitted, R tended to the smaller values 0·070 and 0·060, respectively, and the displacements of the y coordinates tended to zero, that is, y for $M(1)$ and $M(2)$ tended to 0·125, the normal rutile value.

As the scattering factor for Nb^{4+} is about six times larger than that for O^{2-}, the former is predominant in the determination of the atomic positions. If the displacements of atomic positions from the basic rutile positions are denoted by Δx, Δy and Δz and $\Delta x'$, $\Delta y'$ and $\Delta z'$, in the cases of ordinary and subgroup refinements, respectively, two kinds of metal-atom positions may be summarized as follows:

Ordinary refinement, using all the reflections available

$M(1)$ $x_1 = 0{\cdot}125 - \Delta x$, $y_1 = 0{\cdot}125 + \Delta y$, $z_1 = 0{\cdot}5 - \Delta z$
$M(2)$ $x_2 = 0{\cdot}125 + \Delta x$, $y_2 = 0{\cdot}125 - \Delta y$, $z_2 = 0{\cdot}0 + \Delta z$
$\Delta x = 0{\cdot}0087$, $\Delta y = 0{\cdot}0$, $\Delta z = 0{\cdot}022$.

Subgroup refinement

(1) using the *hkl* group

$M(1)$ $x_1 = 0{\cdot}125 - \Delta x'$, $y_1 = 0{\cdot}125 + \Delta y'$, $z_1 = 0{\cdot}5 - \Delta z'$
$M(2)$ $x_2 = 0{\cdot}125 + \Delta x'$, $y_2 = 0{\cdot}125 - \Delta y'$, $z_2 = 0{\cdot}0 + \Delta z'$

(2) using the *khl* group

$M(1)$ $x_1 = 0{\cdot}125 - \Delta x'$, $y_1 = 0{\cdot}125 - \Delta y'$, $z_1 = 0{\cdot}5 - \Delta z'$
$M(2)$ $x_2 = 0{\cdot}125 + \Delta x'$, $y_2 = 0{\cdot}125 + \Delta y'$, $z_2 = 0{\cdot}0 + \Delta z'$
$\Delta x' \simeq \Delta x$, $\Delta y' \simeq 0{\cdot}0005$, $\Delta z' \simeq 0{\cdot}023$.

Relative displacements are shown in Fig. 1. The results for the ordinary refinement are: in the xy plane both x_1 and x_2 deviate significantly from 0·125 (ideal rutile

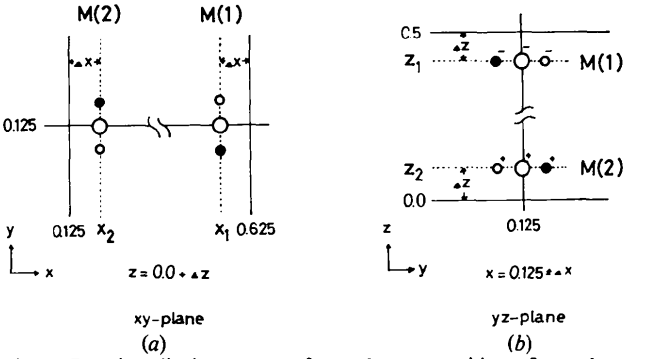

Fig. 1. Relative displacements of metal-atom positions from the basic rutile positions for the ordinary and subgroup refinements of $Nb_{0\cdot96}Ti_{0\cdot04}O_2$: (*a*) xy plane, $z = 0{\cdot}0 + \Delta z$; (*b*) yz plane, $x = 0{\cdot}125 \pm \Delta x$. ○ Ordinary refinement, using all the reflections; ○ subgroup refinement, using *hkl* group; ● subgroup refinement, using *khl* group.

value); in the yz plane z_1 and z_2 depart significantly from 0·5 and 0·0, respectively, giving alternately short and long distances between $M(1)$ and $M(2)$ along z. For the subgroup refinements, displacements of the y coordinate, $\Delta y'$, for each group of hkl and khl are in opposite directions and are mirror symmetric with each other.

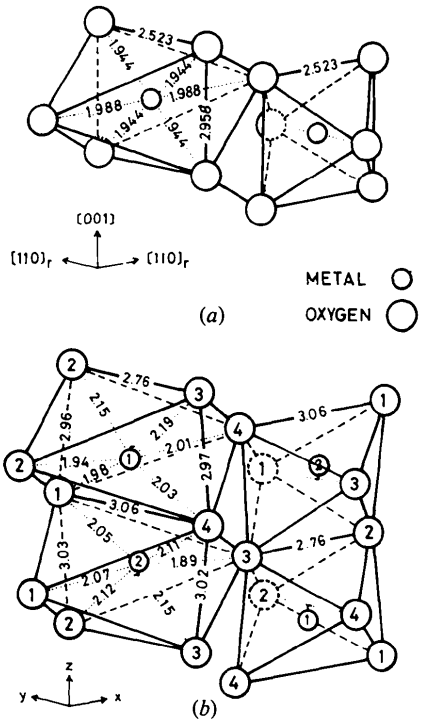

Fig. 2. Structural units and interatomic distances (Å) for (*a*) TiO_2 and (*b*) NbO_2.

Table 7. *Interatomic distances* (Å) *for* $Nb_{1-x}Ti_xO_2$

Maximum standard errors (2σ) found ($\times 10^3$) for: M–M, 9; M–O, 34; O–O, 44.

	Composition x			
	0·00	0·04	0·09	0·20
$M(1)$–$M(2)$	2·707	2·740	2·755	2·888
$M(1)$–$M(2)$	3·298	3·276	3·231	3·112
O(1)–O(4)	3·055	3·048	2·974	2·879
O(2)–O(3)	2·764	2·730	2·743	2·748
$M(1)$–O(1)	1·977	2·026	2·002	2·072
–O(2)	2·147	2·136	2·117	2·036
–O(3)	2·196	2·152	2·126	2·047
–O(4)	2·029	2·019	2·008	2·064
O(1)–O(2)	2·962	2·979	2·953	2·999
O(3)–O(4)	2·967	2·977	2·950	2·992
$M(2)$–O(1)	2·051	2·080	2·044	1·999
–O(2)	2·119	2·114	2·114	2·107
–O(3)	2·145	2·127	2·120	2·115
–O(4)	2·109	2·075	2·056	2·023
O(1)–O(2)	3·026	3·029	3·022	3·001
O(3)–O(4)	3·022	3·027	3·025	3·008
$M(1)$–O(2)	1·939	1·943	1·942	1·991
–O(4)	2·007	2·025	2·025	1·978
$M(2)$–O(1)	2·074	2·011	2·040	2·012
–O(3)	1·886	1·928	1·928	1·955

The structural unit of the rutile structure is an octahedron, in which a metal atom is surrounded by six O atoms. Strings of MO_6 octahedra extend along c sharing a common edge. The neighbouring strings share a common corner of an octahedron, thus forming the three-dimensional structure. In an ideal rutile structure, such as TiO_2 [Fig. 2(*a*)], the metal atoms are equidistant and line up in a straight line along c. In a distorted rutile, such as NbO_2, interatomic distances between the central metal atoms are alternately shorter and longer and the O-atom octahedra are accordingly distorted [Fig. 2(*b*)]. M–M, M–O and O–O distances determined for $Nb_{1-x}Ti_xO_2$ are summarized in Table 7. The values given in Table 7 were obtained from the coordinates given in Table 2. Fig. 2(*a*) and (*b*) shows, for comparison, corresponding distances for TiO_2 and NbO_2, respectively.

Results and discussion

(*a*) *Structure analysis*

PAT (1976) maintained that the deviations of atomic coordinates in NbO_2 from those in the basic rutile structure, especially the deviations of the O atoms, could only be determined by neutron diffraction. However, the present X-ray experiment has also succeeded.

The LT phase of $Nb_{1-x}Ti_xO_2$ belongs to the space group $I4_1/a$. Table 6 shows that a systematic discrepancy between F_o and F_c is observed for superlattice reflections with $h, k = 2n + 1$ and $l = 2n$, that is, while theoretically $F_c(hkl) \neq F_c(khl)$ for crystals belonging to $I4_1/a$, experimentally $F_o(hkl) \simeq F_o(khl)$. Because of this discrepancy, R is rather large, 0·12, in the ordinary refinement (Table 2). By omitting the reflections with a large value of ΔF, R can be considerably improved, for example, from $R = 0{\cdot}14$ to 0·038 for NbO_2. However, such a refinement brings about no appreciable change in the atomic coordinates of $M(1)$ and $M(2)$, while the temperature factors are reduced appreciably. Here, the collected reflections were divided into two subgroups, *i.e.* hkl and khl, and two independent refinements were carried out (Table 4). The change in the y coordinate for both $M(1)$ and $M(2)$ in one subgroup refinement was found to be in the opposite direction with respect to the corresponding movement in the other subgroup refinement. Thus, it may be considered that in the ordinary refinement, the least-squares procedure has smeared out these opposing movements, giving $\Delta y = 0$ (Table 2, NbO_2 and $Nb_{0.96}Ti_{0.04}O_2$). In this respect, F_o and ΔF_o syntheses using the three kinds of atomic parameters, those obtained by the ordinary, the hkl subgroup and khl subgroup refinements, were calculated. It was hoped that by using these procedures, some appreciable

improvement in R would occur (Koto, 1977); however, the results gave no such improvement.

(*b*) *Structural features: molecular-chain model*

As stated above, the systematic discrepancy between F_o and F_c of the superlattice reflections $h, k = 2n + 1$ and $l = 2n$, originates from the fact that the shifts of $M(1)$ and $M(2)$ along y are in opposite directions for the different subgroup refinements. Actually, the absolute values of these shifts are very small (at most 0·007 Å). Therefore, for the purpose of the discussion of the bond characters in $Nb_{1-x}Ti_xO_2$, it may suffice to make use of the atomic coordinates obtained by the ordinary refinement. In the following we discuss the bonding character in $Nb_{1-x}Ti_xO_2$. The ionic radii of Ti^{4+}, Nb^{5+} and O^{2-} are 0·60, 0·67 and 1·46 Å [Zachariasen's values quoted by Kittel (1956)], respectively. With these values, Nb–O and O–O distances in NbO_2 are 2·13 and 2·92 Å, respectively. The observed distances in the yz plane and along x are shown in Fig. 2(*b*) and Table 7. We may consider the difference between ionic bond length and the actual bond length to be a covalent contribution. Then, for the x direction, the covalent contribution is much larger in $M(1)$–O(2) or $M(2)$–O(3) bonds than in $M(1)$–O(4) or $M(2)$–O(1) bonds. $M(1)$–$M(2)$ distances along c are alternately 2·707 and 3·298 Å. The latter fact substantiates the existence of a direct covalent bond between $M(1)$–$M(2)$. In Fig. 3(*a*), the shorter and longer $M(1)$–$M(2)$ distances for $Nb_{1-x}Ti_xO_2$ are shown as a function of x. With increasing x, both distances approach each other and coincide at $x \simeq 0{\cdot}3$, giving 3·00 Å. On the other hand, the O(1)–O(4) distance decreases rapidly, while O(2)–O(3) remains practically unchanged with increasing x. The former value approaches the latter until they coincide at $x \simeq 0{\cdot}3$. At this composition the mean value of the M–O distances for the x direction appears to be 1·98 Å [Fig. 3(*b*)]. These variations in atomic distances with x are in accordance with the fact that $Nb_{1-x}Ti_xO_2$ takes a normal rutile structure for $x \simeq 0{\cdot}3$.

The O(1)–O(4) bonds (along y) are almost at right angles to the shorter $M(1)$–$M(2)$ bonds (along z). Compared to O(2)–O(3), the O(1)–O(4) distance is increased; this increase occurs because of the strong $M(1)$–$M(2)$ bond. The distortion of the MO_6 octahedron is taken to be caused mainly by the strong covalent-pair bond, $M(1)$–$M(2)$. In the NbO_2 structure, by joining the shortest bonds along x, one obtains parallel, wavy molecular chains, Fig. 4. Similar chains are also formed in the y direction. The chains along x and y never intersect.

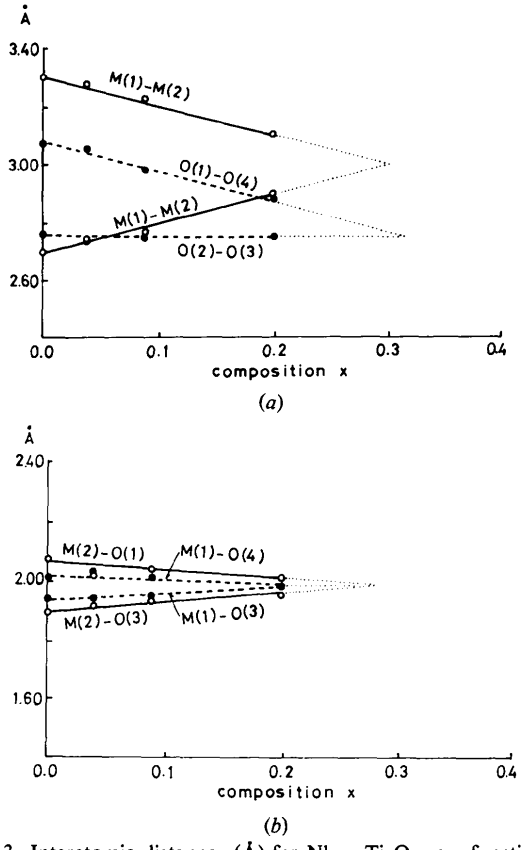

Fig. 3. Interatomic distances (Å) for $Nb_{1-x}Ti_xO_2$ as a function of composition x: (*a*) M–M and O–O distances in the yz plane and (*b*) M–O distances along x.

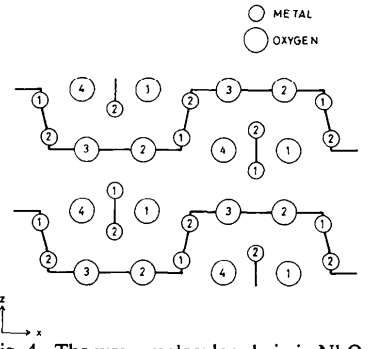

Fig. 4. The wavy molecular chain in NbO_2.

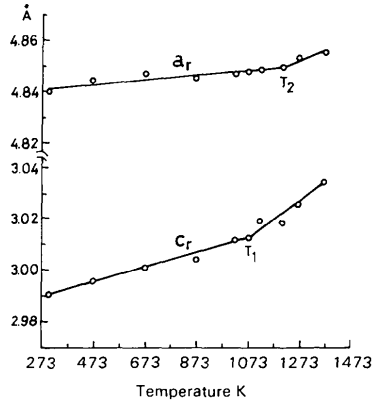

Fig. 5. The temperature variation of lattice parameters. T_1 and T_2 are the phase-transition points for c_r and a_r respectively.

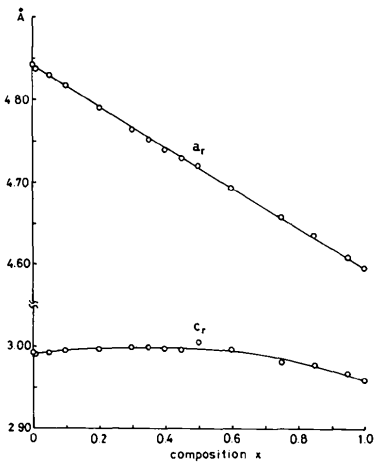

Fig. 6. Lattice parameters for $Nb_{1-x}Ti_xO_2$ at room temperature.

Whereas TiO_2 has a cleavage along z reflecting the shortest bonds lying in the $(1\,1\,0)_r$ plane (corresponding to the xz plane of NbO_2), the fact that NbO_2 has no preferential habit seems to support the existence of the wavy molecular chains in the latter, which three dimensionally reinforce the crystal.

The linear expansion coefficients along a_r and c_r as a function of temperature for NbO_2 have been reported by Sakata (1969*a*). A detailed re-examination of Sakata's data has been carried out and the results are shown in Fig. 5. Changes in gradient on the c_r and a_r curves occur at $T_1 = 1073$ and $T_2 \simeq 1173$ K, respectively. T_1 corresponds to the phase-transition temperature T_c deduced from the electrical conductivity, magnetic susceptibiity and DTA, but T_2 is much higher than T_c. Sakata (1969*a*) has pointed out that the structural phase transition is not complete at T_c. In this respect, it might be considered that the phase transition from the deformed into the normal rutile-type structure in NbO_2 would proceed through an intermediate phase existing between T_1 and T_2. Tolédano & Tolédano (1977) have also asserted the existence of such an intermediate phase in NbO_2. It may be that at T_1 the Nb—Nb bonds break, then at T_2 the re-adjustment in the intramolecular Nb—O—O—Nb distances takes place.

In $Nb_{1-x}Ti_xO_2$, a_r decreases with increasing composition x, while c_r remains unchanged up to $x \simeq 0{\cdot}6$, Fig. 6. For $0 < x < 0{\cdot}1$, T_c decreases from 1073 to 873 K (Sakata, 1969*c*). On the other hand, as shown in this report, the longer and shorter Nb—Nb distances along c coincide at $x \simeq 0{\cdot}3$. The behaviour of c_r is caused, presumably, by the following three effects. Firstly, the dimerization of the Nb—Nb bonds increases, which results in a lengthening of c_r. Secondly, the size effect of Ti^{4+} causes reduction of c_r. Thirdly, T_c decreases with increasing x, and approaches room temperature at $x \simeq 0{\cdot}3$.

The author thanks Professor T. Sakata of the Faculty of Science, Science University of Tokyo, for helpful comments and discussions, and Professor Y. Iidaka of the Faculty of Pharmacy, Tokyo University, for use of the diffractometer and for helpful discussions and suggestions. All computations were carried out at the Computation Centers of Tokyo University, with *MINEPAC* (M. Miyamoto & H. Takeda).

References

BÉLANGER, G., DESTRY, J., PERLUZZO, G. & RACCAH, P. M. (1974). *Can. J. Phys.* **52**, 2272–2280.

JANNINCK, R. F. & WHITMORE, D. M. (1966). *J. Phys. Chem. Solids*, **27**, 1183–1187.

KITTEL, C. (1956). *Introduction to Solid State Physics*, 2nd ed., p. 81. New York: John Wiley.

KOTO, K. (1977). Private communication.

MAGNÉLI, A., ANDERSSON, G. & SUNDKVIST, G. (1955). *Acta Chem. Scand.* **9**, 1402.

MARINDER, B. O. (1963). *Ark. Kemi*, **19**, 435–446.

PYNN, R. & AXE, J. D. (1976). *J. Phys. C*, **9**, L199–L202.

PYNN, R., AXE, J. D. & RACCAH, P. M. (1978). *Phys. Rev. B*, **17**, 2196–2205.

PYNN, R., AXE, J. D. & THOMAS, R. (1976). *Phys. Rev. B*, **13**, 2965–2975.

RAO, C. N. R., RAMA RAO, G. & SUBBA RAO, G. V. (1973). *J. Solid State Chem.* **6**, 340–343.

RÜDORFF, W. & LUGINSLAND, H. H. (1964). *Z. Anorg. Allg. Chem.* **334**, 125–141.

SAKATA, K. (1969*a*). *J. Phys. Soc. Jpn*, **26**, 582.

SAKATA, K. (1969*b*). *J. Phys. Soc. Jpn*, **26**, 867.

SAKATA, K. (1969*c*). *J. Phys. Soc. Jpn*, **26**, 1067.

SAKATA, K., NISHIDA, I., MATSUSHIMA, M. & SAKATA, T. (1969). *J. Phys. Soc. Jpn*, **27**, 506.

SAKATA, T., SAKATA, K., HÖFER, G. & HORIUCHI, T. (1972). *J. Cryst. Growth*, **12**, 88–92.

SAKATA, T., SAKATA, K. & NISHIDA, I. (1967). *Phys. Status Solidi*, **20**, 155–157.

SHAPIRO, S. M., AXE, J. D., SHIRANE, G. & RACCAH, P. M. (1974). *Solid State Commun.* **15**, 377–381.

SHIN, S. H., HALPERN, T. H. & RACCAH, P. M. (1975). *Mater. Res. Bull.* **10**, 1061–1066.

TOLÉDANO, P. & TOLÉDANO, J. C. (1977). *Phys. Rev. B*, **16**, 386–407.